Chapter

Time-Domain Simulation of Microstrip-Connected Solid-State Oscillators for Close-Range Noise Radar Applications

Vladimir Yurchenko and Lidiya Yurchenko

Abstract

We develop time-domain approach for simulation of microstrip-connected extremely-high frequency (EHF) solid-state oscillators for close-range radars, including ultrashort-pulse, ultrawide-band (UWB), and noise radars. The circuits utilize high-speed GaN-based active devices such as Gunn diodes (GD) and resonant-tunneling diodes (RTD) capable of operating with enhanced power output. Microstrip interconnects produce time-delay coupling in the system that can create a complicated nonlinear dynamics of oscillations. The circuits can generate self-emerging trains of ultra-short EHF pulses emitted into an open microstrip section for further radiation. The arrays of active devices connected in either parallel (star-case) or series (ladder-case) type of circuits were simulated. Options for generation of chaotic signals in this kind of systems have been considered. An infrared-microwave (IR-EHF) oscillator linked to the resonant antenna was simulated. The oscillator consists of an RTD-driven laser diode (LD) joint to the EHF resonant antenna with a short piece of microstrip section. The oscillator can generate both the EHF pulse radiation and the EHF modulated IR pulses. Both kinds of radiation can be emitted in the free space as the trains of correlated IR-EHF radar pulses. Arrays of oscillators can be used for enhancing the power output of the system.

Keywords: time-domain simulations, solid-state oscillator, THz, millimeter wave, time-delay, chaos, distributed systems, active devices, Gunn diode

1. Introduction

Emerging demands for the EHF oscillators capable of generation of ultra-short pulses and complicated waveforms including chaotic oscillations lead to the development of new approaches to the design and analysis of oscillator systems. The EHF oscillators are of interest for numerous applications. Significant part in these applications belongs to radar systems including, particularly, close-range and noise radars, which require ultrashort-pulse, ultrawide-band, and noise oscillation sources [1, 2]. There are different kinds of the EHF oscillators ranging from microwave power tubes (klystrons, gyrotrons, backward-wave tubes, etc.) to solid-state

devices (transistor-based circuits, Gunn diodes, etc.) [3, 4], of which only the latter are discussed in this chapter.

Design of oscillators and circuits is conventionally made in frequency domain. A significant contribution to the design was made by Kurokawa [5, 6] through advancing the negative resistance oscillator concepts and developing stability analysis methods. He developed the impedance approach to the analysis of oscillator systems that makes it possible to design, in particular, multi-device circuits with spatial power combining [6].

Numerous advances to the design and analysis of oscillators have been made in the following years [7–9]. Significant developments are the extension of the frequency-domain analysis for the account of nonlinear characteristics of active devices [7], the analysis of different impedance and admittance formulations in the oscillator design [8], the application of hybrid harmonic-balance approach [9], etc. A vast literature exists on the design of oscillators with frequency-domain methods.

In this line, time-domain oscillator analysis is not a common practice. In order to deliver essential information about the oscillators and their dynamics, time-domain analysis requires huge amount of numerical simulations of complicated oscillatory systems, which have to be made in a broad range of oscillator parameters.

Despite this difficulty, there are circumstances when such an analysis is a necessity, since no alternative approach can provide adequate information on the oscillator dynamics in the relevant cases. These are the cases when ultrashort-pulse, ultrawide-band, and noise oscillation signals have to be generated [1, 2]. The problem exacerbates when signals should have extremely broad frequency spectrum extended in the EHF and THz bands.

Design of generation and transmission systems for this kind of signals inherently requires the time-domain approach [10]. For passive components like antennas, valuable contributions to mathematics of time-domain modeling that concerns ultrashort-pulse and ultrawide-band signals have been made [11, 12]. The oscillators are, however, much too complicated unstable and nonlinear systems for the efficient simulations. Nonetheless, time-domain modeling is, in fact, the most meaningful approach to the design of oscillators generating this kind of signals [13, 14], though the frequency-domain methods can also be helpful [15].

A practical way of making progress in the analysis of these oscillators is to consider simplified models, which, despite their simplicity, represent essential features of real systems. An important feature of oscillators in the EHF and THz bands is their distributed character. Even though active devices and other discrete elements may be small, their assembly into an operating circuit with extended interconnects, resonators, and antenna components makes the entire system to be comparable to the radiation wavelength.

Thus, time delay arises, essentially, due to the delayed coupling between the components that makes the circuit to operate as a distributed system. Time delay leads to complicated dynamics and, often, to the dynamical chaos in nonlinear systems [16] that makes time-delay oscillators to be attractive devices for numerous applications.

A particularly useful simplification arises when making clear distinction between discrete and distributed components and defining the model where discrete units (circuit elements or blocks of elements) are joined by transmission lines (waveguides, microstrips, etc.) in a way that qualitatively represents the actual connectivity of components in the entire system. Then, discrete blocks can be simulated by local equations in time domain and the effects of transmission lines can be accounted by readily available analytic solutions of simplified wave equations. The entire system is then suitable for reasonably efficient time-domain simulations.

We applied the approach to the time-domain analysis of a range of different distributed circuits with active devices where we assumed that the transmission lines are, typically, the microstrip sections and the active devices are either the Gunn diodes or the resonant tunneling diodes in that or another circuit [17–25]. Transmission lines introduce time delays in the coupling between discrete units that makes the entire circuits to operate as the time-delay oscillators.

Our microstrip-based oscillator models are qualitatively different from other time-delay oscillators usually considered [4]. The difference is that, instead of using pre-defined phase delays in the feedback circuits, we consider time-delays that emerge self-consistently as a result of backward and forward EM wave propagation along the transmission lines with account of their scattering and interference with other process, making the effects particularly complicated. The systems take into account the fact that, at the frequencies of the EHF and THz range, i.e., for the millimeter and sub-millimeter waves, time-delays become unavoidable due to the extended structure of oscillator circuits.

The following Sections present overview of basic results obtained in our time-domain simulations of extended transmission line time-delay oscillators.

2. Kinds of circuits and forms of oscillations

We consider solid-state oscillators that can be presented as a combination of both the lumped units (lumped circuit blocks) and distributed microstrip sections (pieces of transmission lines) of different configurations. Microstrip sections provide interconnects between the lumped units and produce time-delay in the coupling between different circuit components.

The lumped units are built up of discrete active and passive devices whose interconnects within each block are of infinitesimal length as compared to the typical wavelength λ_0 of the electromagnetic (EM) waves emerging in the system as a result of complicated self-oscillation process. For this reason, there is no time delay arising due to signal propagation between discrete elements, including active devices, within each lumped unit. There are neither special time-delay devices of other kinds included in the lumped units. The units being used are, in fact, rather simple pieces of circuits made up of active devices (Gunn diodes, avalanche diodes, resonant tunneling diodes) and passive elements (resistors, capacitors, and inductances).

The distributed sections are the pieces of microwave transmission lines (e.g., microstrip lines as representative elements or any other waveguide structures). Transmission lines (TL) provide time-delay coupling between the lumped units. Time delay appears in the coupling between the lumped units connected by any TL section because of some time needed for the EM wave propagation along the section between the units. The time delay has to be accounted in the analysis when the length d_n of the relevant TL section identified by index n is not too small as compared to the typical wavelength λ_0 of the EM waves propagating along the section.

Schematics of a few circuits being considered are presented in Sections 5, 7, and 8 below. Depending on the kind of circuits, different types of nonlinear oscillation can be excited in time-delay systems. The key elements in these distributed systems are the active blocks that contain one or another kind of solid-state active devices.

We consider the EHF solid-state devices such as Gunn diodes or the resonant tunneling diodes (RTD) that can operate in a broad range of frequencies varying from, essentially, 10GHz to about 1 THz and more. The operation of these devices and oscillators is best understood in terms of the negative resistance oscillator

concepts [7, 8]. Typically, we consider the Gunn diode circuits in our models, though one example of RTD system is discussed in the Section 8. In practice, the most common are the GaAs Gunn diodes but GaN devices are now of greater interest due to their potential for high-power and high-frequency operation.

The Gunn diodes are simulated using the approximation of limited space-charge accumulation (LSA) mode. In this mode, the strong-field domain in the Gunn diode is bounded to the surface electric contact and can only oscillate near the contact rather than travel through the entire structure. Then, the oscillation frequency of the Gunn diode can vary in a broad range and achieve rather high values.

Using the LSA approximation, the device operation can be described in terms of the given current-voltage characteristics with negative differential resistance (NDR) region. In this model, the current-voltage characteristics of typical Gunn diodes, e.g., GaAs diodes, can be presented in the following form [17–24].

$$G(e) = G_0 F(e) \tag{1}$$

where $G(e)$ is the diode current in relative units, $F(e)$ is the function defining the shape of the current-voltage characteristics, $G(e) = G_0 I(e)/I_0$, $G_0 = Z_0 I_0/V_0$, $e = V/V_0$, I_0 and V_0 are the scaling factors for the diode current $I(e)$ and voltage V, respectively, and Z_0 is the microstrip wave impedance (I_0 and V_0 parameters are specified by the Gunn diode threshold current and voltage, respectively).

The Gunn diode self-excitation begins when the voltage V falls in the NDR region. We accept the intrinsic impedance of microstrip lines to be $Z_0 = 50$ Ohm and use $G_0 = 2$ as a typical Gunn diode parameter (typically, $I_0 = 0.2$A, $V_0 = 5$ V for GaAs and $I_0 = 1.2$ A, $V_0 = 30$ V for GaN structures).

The formulation in terms of the current-voltage characteristics, which is typical for the LSA approximation, means that the diode is capable of instant response to any external signal. The operation of such a diode is, formally, not limited from above by any high frequency value. In reality, though, the high-frequency operation is limited by the diode intrinsic capacitance C and the inductance L of the mounting contacts. These parameters define the natural intrinsic frequency of the Gunn diode when it is mounted in one or another way in the transmission line. Typically, due to quite noticeable value of inductance, this intrinsic frequency is lower than the highest frequency accessible for the diode operation.

In our models, we consider both kinds of approximations when the Gunn diode is either not limited in the oscillation frequency or, on the contrary, is characterized by intrinsic capacitance and inductance, which impose the limit on the diode operation frequency. In the latter case, the intrinsic capacitance and inductance are defined as the effective components directly connected to the Gunn diode within the lumped active unit.

Early models, for simplicity, did not account for the diode capacitance and inductance, thus, ignoring the diode frequency limit. The approximation allowed us to significantly simplify the original problems and reduce them to the forms which are more accessible for numerical simulations. In this way, we could consider self-excitation and nonlinear dynamics of the EM field oscillations in a closed two-dimensional (2D) rectangular cavity with an active wall [17, 18] and self-emergence of trains of pulses emitted from one-dimensional (1D) cavity with such a wall on the one side and a dielectric plate as a semi-transparent mirror on the other side that makes the cavity an open resonator [19]. These simulations are discussed in Section 4.

Later models took into account the intrinsic frequencies of active devices. When applied to 1D microstrip circuits and the networks of circuits with either parallel or series connections of branches, we could observe and analyze a series of new effects

in self-oscillations of these circuits [20–25]. The circuits and relevant effects are considered in Sections 5–8.

The dominant effect in these circuits, apart from conventional continuous wave (CW) generation, is the excitation of trains of short radio-frequency (RF) pulses. When using high-speed devices such as GaAs and GaN Gunn diodes in circuits with proper other parameters such as a high resonator frequency and a short length of microstrip sections, one can achieve self-excitation of short trains of ultra-short EHF pulses, which are emitted into an infinite section of another transmission line. Self-developing transitions between either the CW or pulse modes of EHF oscillations are possible, which depend on both the operation conditions and prehistory of oscillations, thus, revealing the hysteresis and bistability effects in the time-delay EHF oscillators being considered.

3. Mathematical models and simulation techniques

Time-domain analysis of nonlinear oscillator systems is based on computer simulations for the numerical solutions of oscillatory equations. Typically, ordinary differential equations (ODE) for lumped systems or partial differential equations (PDE) for distributed structures are in use. For more complicated cases, integral-differential, difference-differential, difference-integral-differential, and other kinds of equations may be needed for the adequate modeling of real oscillator systems. The term difference-differential means the equations that account for the finite delay in their arguments that appear in some terms of the equations. The equations of this kind are also called the equations with deviating arguments.

In our models, the delay in the electromagnetic coupling between spatially separated blocks creates multiple time delays in the evolutionary equations that can be derived for the entire oscillator system. The equations are formulated for the electromagnetic field, current, and voltage quantities as functions of time and spatial coordinates in the given circuits. Using various transformations, the equations are reduced to some other forms mentioned above to make their numerical solution more accessible.

Specific examples of equations obtained in this way for some of the models are presented in the following Sections. Typically, the equations are reduced to one or another version of a set of ODEs with time-delay arguments in their terms that describe the EM wave coupling in the distributed microstrip circuits.

For the accurate solution of these equations, we applied a highly efficient and reliable Dormand-Prince method of the (5,3) order of accuracy [26]. A publicly available software code of the method was amended with our extension that provided the dynamical storage of dense output of a solution in a long period of time in the past so as all the time-delayed values were available.

Since the past values are requested by solver at some unknown time nodes in the storage domain that may exceed the formal time-delay value, we created sufficiently large storage domain, applied polynomial interpolation of a high and controllable accuracy that uses a big domain and many nodes around the requested node, and provided a special control that no limitations are broken.

Thus, we obtained a unique, highly accurate and reliable software tool for time domain simulations of complicated nonlinear dynamics of time-delay oscillators that may exhibit dynamical chaos and other unstable transient, oscillatory, and evolutionary developments. The tool appeared to be highly efficient for solving the time-domain problems arising for our models of time-delay oscillatory systems.

More generic software tools could also be used for time-domain simulations of oscillator circuits. At present, SmartSpice simulation software is available for the

engineering applications of time-domain circuit analysis [27] though applicability of generic techniques for time-delay problems and complicated circuits is limited.

The other circuit models that assumed an instant response of active devices (excluding the case of 2D cavity) lead to the difference-delay equations rather than time-delay ODEs. These equations are solved by direct iteration process.

In all the problems considered, the initial conditions were spatially uniform steady-state solutions that exist at the given initial parameters including the bias voltage V_B regardless whether the solution is stable or unstable. In case of a stable initial condition, when the device voltage V_G is out of the NDR region, the bias V_B is altered with a certain rise time so as to set the device voltage V_G in the NDR domain where the oscillations begin. In the other cases, when the initial condition is unstable due to the initial device voltage V_G is set in the NDR region, a minor fluctuation of the bias voltage is introduced that initiates the circuit self-excitation process.

4. Early models, dynamical chaos, and pulses

The early models assumed an instant response of active devices. In this way, they ignored any possible frequency limitations imposed by the limited operation speed of active devices characterized by the relevant intrinsic frequency f_G. So, any specific frequencies of emerging oscillations were defined by the passive circuit components and nonlinear character of the entire oscillator system.

The first model [17, 18] is presented by the 2D rectangular cavity ($0 < x < D$, $0 < z < A$) with perfectly conducting walls, of which one wall ($x = D$) is covered with an active semiconductor layer specified by nonlinear current-voltage ($I - V$) characteristics with NDR domain as defined in Eq. (1). The active layer is used as an approximation for, e.g., a dense array of active devices such as the Gunn diodes placed on one of the cavity walls inside the cavity. The quantities of interest are the electric field in the cavity $E_z(x, z, t)$ and the average field $U(t)$ at the active layer when the external voltage is applied to active devices and the electric field is set in the NDR region. Self-excitation is developing in the system when a minor fluctuation of the EM field is introduced in the cavity.

The evolution of self-excitation may occur in a different manner depending on the system parameters. An essential parameter is the coupling coefficient G_0 representing the strength of coupling of the electric field at the cavity wall $x = D$ with active devices and, implicitly, the maximum electric current in the active layer. In this way, the coefficient defines the EHF power that can be generated by active devices.

The main result obtained in this model is the emergence of the dynamical chaos of the EM field in the cavity when the coupling coefficient G_0 is made sufficiently large [17, 18]. To identify the chaos, three basic criteria have been used: (a) specific structure of the Poincare sections, (b) broad-band character of the power spectrum of oscillations and (c) sensitive dependence of solutions on the initial conditions. In addition, the wavelet analysis was applied to study the evolution of the excited field. The Morlet wavelets have been used to scale the frequency band $0.4 \leq fD/c \leq 6.4$ in the time interval of $375 \leq ct/D \leq 400$ where c is the speed of light.

Most of simulations were made with a square cavity ($A = D$). The square cavity often generated chaotic dynamics of the $E_z(x, z, t)$ field whereas a shorter cavity (e.g., $A = 0.8D$) showed a greater stability. Yet, the main factor controlling the emergence of chaos is the coupling coefficient G_0. When the coefficient is small, e.g., $G_0 = 0.1$ in case of the square cavity, only regular and, essentially, single-frequency oscillations appear. At the intermediate coupling, e.g., $G_0 = 1$, the

co-existence of multi-frequency and chaotic generation is observed. Finally, at the very strong coupling when, e.g., $G_0 = 30$, chaotic oscillations dominate.

Simulations in this 2D model were made using the series expansion of the cavity field in spatial modes with time-dependent expansion coefficients in a way, which is conceptually similar to formulations developed in [11]. In this way, a set of nonlinear ODEs was obtained for the expansion coefficients as unknown functions. The active layer $I - V$ characteristics entered this formulation through the boundary conditions imposed at the active wall $x = D$, where they played a role of nonlinear impedance boundary conditions formulated in time domain. Other approaches using, e.g., Green's function formulations and taking into account non-instant response of active devices, should also be explored.

The second model [19] is formulated as a 1D open-cavity problem where the 1D cavity $(0 < x < D)$ is formed by the first wall at $x = D$, which is covered with the same instant-response active layer as explained above, and the second wall at $x = 0$, which is made as a thin dielectric layer of thickness d $(-d < x < 0)$ that operates as a resonant semi-transparent mirror for the cavity field.

In this case, the problem formulated for the electric field $E_z(x,t)$ that exists in both the cavity, the dielectric mirror, and the half-space outside the cavity, is reduced to a single, though, complicated, delay-difference equation with multiple time delays, which is formulated for the auxiliary function $g(\tau)$ where $\tau = ct/D$ is the time variable t in the relative units. The other functions of interest such as the oscillation waveform $U_1(\tau)$ emitted through the dielectric mirror are also defined via the function $g(\tau)$ [19].

The main result obtained for these structures is that, typically, a train of the EHF pulses is self-excited in the 1D oscillator. The basic frequency of the EHF oscillations in these pulses is defined by the thickness d and refractive index n of dielectric mirror. No intrinsic frequency of active devices is present in this problem since active devices are specified by an instant response and impose no frequency limits on the emerging self-oscillations. In other cases, depending on the parameters, trains of baseband pulses with no carrier frequency are self-excited.

Characteristic frequencies of the EHF pulses emerging in these structures would be, e.g., $f = 64$ GHz ($\lambda_0 = 4.7$ mm) at the pulse duration $t_P = 0.17$ ns (the pulse frequency width $f_P = 1/t_P = 6$ GHz) and the pulse repetition frequency $f_{REP} = 3$ GHz should the devices were capable of operation at these frequencies, the dielectric mirror made of a MgF_2 wafer of thickness $d = 1$ mm having the refractive index $n = 2.345$ at the extremely low loss tangent $\tan(\delta) = 5 \cdot 10^{-5}$ [28], and the resonator length chosen to be $D = 25$ mm.

5. Active circuit with a remote resonator antenna

The model that removes an essential limitation of instant response of active devices was investigated in detail in [20]. The model is rigorously formulated in terms of the 1D microstrip distributed circuit with spatially separated active and passive components, **Figures 1** and **2**.

The circuit consists of four basic parts which are (i) an active block G_1 made as a lumped unit with Gunn diode as an active device, (ii) a remote resonator A_0 (we assume this is an LC circuit implemented as a lumped block), (iii) a section of microstrip line of length D connecting the active block and the resonator (this is a distributed part of the circuit), and (iv) an infinite section of microstrip line connected to the resonator. The latter allows the waves excited in the circuit to be radiated towards the infinity, thus, simulating the radiation into the free space, with resonator block A_0 operating also as an antenna unit.

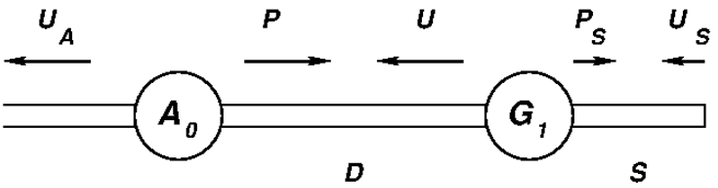

Figure 1.
Schematics of a microstrip circuit with Gunn diode active block G_1 and a resonator antenna block A_0.

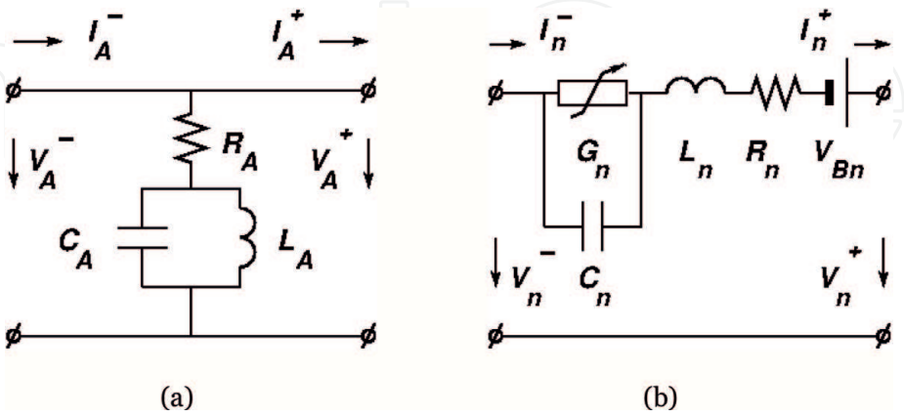

Figure 2.
Schematics of (a) passive and (b) active blocks of **Figure 1** *($n = 1$).*

Figures 1 and **2** show a more generic version of the system considered in [20]. The system of a generic kind includes the stub of the length S that facilitates the emergence of self-oscillations and the lumped circuit resistors R_A and R_n $(n = 1)$ that simulate absorption losses (equations below and the results are presented for a simpler case of $S = 0$ and $R_A = R_1 = 0$).

The governing differential equations and boundary conditions are obtained by applying the wave equations to the transmission line sections and the Kirchhoff circuit equations to the diode and resonator blocks. The wave equations describe the voltage waves P, U, and U_A that propagate to the right and to the left in the microstrip sections as shown in **Figure 1**, respectively. They are the unknown functions to be found.

The Kirchhoff equations define boundary conditions imposed at the contact points of both the Gunn diode and resonator circuits. They are formulated in terms of the voltage and current values at the contact points $e^{\pm}$, $e_A^{\pm}$, $i^{\pm}$, $i_A^{\pm}$, which are defined via the unknown waveforms P, U, and U_A. The radiation boundary condition is applied that ensures no incoming waves in the open microstrip section (microstrips are assumed lossless and free of dispersion).

The initial condition is imposed as the state of no oscillations when the diode voltage is set outside the NDR region by the source voltage e_{B_0}. Self-excitation appears when the Gunn diode is driven into the NDR region by increasing (decreasing) the source voltage $e_B(\tau)$ with a certain rise (fall) time T_R (T_F).

The time and space variables are used in relative units $\tau = ct/a$ and $x = \tilde{x}/a$ where t and $\tilde{x}$ are the original time and space variables, respectively, c is the speed of wave in the microstrip line, $d = D/a$ is the length of microstrip section in relative units, and a is the spatial scale used for normalization.

The equations for this model are reduced to a set of ODEs with time delays

$$U''(\tau) + U''(\tau - 2d) - U_A''(\tau - d) + \omega_L\left[U'(\tau) - U'(\tau - 2d) + U_A'(\tau - d) + e_B'(\tau)\right] + \omega_G^2[U(\tau) + U(\tau - 2d) - U_A(\tau - d) - G(e(\tau)) + G(e_0)] = 0, \tag{2}$$

$$U_A^{''}(\tau) + 2\omega_{C_A}\left[U_A'(\tau) - U'(\tau - d)\right] + \omega_A^2 U_A(\tau) = 0, \tag{3}$$

$$\begin{aligned} e(\tau) = e_B(\tau) - U(\tau) + U(\tau - 2d) - U_A(\tau - d) \\ - \omega_L^{-1}[U'(\tau) + U'(\tau - 2d)] - U_A'(\tau - d)] \end{aligned} \tag{4}$$

where $U(\tau)$ and $U_A(\tau)$ are the unknown wave functions, $e(\tau)$is the Gunn diode voltage at the time τ, $\omega_L = aZ_0/cL$, $\omega_{C_A} = a/cZ_0C_A$, $e_0 = e_{B_0}$, $\omega_G^2 = (a/c)^2/LC$, $\omega_A^2 = (a/c)^2/L_AC_A$, and $G(e(\tau))$ is the Gunn diode current defined by Eq. (1). Here, index A denotes the values related to the resonator antenna block, index $n = 1$ is dropped, and the other related angular frequencies are $\omega_{L_A} = {\omega_A}^2/\omega_{C_A}$ and $\omega_C = {\omega_G}^2/\omega_L$, respectively.

6. Bistability, hysteresis, and trains of the EHF pulses

Simulations of oscillators with active circuits and remote resonator antennas revealed the existence of two oscillation modes, of which one mode is the CW oscillations and the other is the trains of the EHF pulses. The emergence of one or another oscillation mode depends on the bias voltage of the Gunn diode circuit. The EHF pulse mode arises when the Gunn diode operating voltage V_{GO} exceeds the lower bound V_1 of the NDR region but the excess is not significant so as the voltage V_{GO} does not fall deep in the NDR region. The CW oscillations, on the contrary, appear when the operating voltage V_{GO} is set deep in the NDR region [20].

An important feature of the effect is the co-existence of both the pulse and the CW modes of oscillations in some range of operating voltages. The oscillator can generate either the EHF pulses or CW oscillations at the same operating voltage V_{GO} when the latter falls in an intermediate domain $V_{B1} < V_{GO} < V_{B2}$ (PC-domain) inside the NDR region $V_1 < V_{GO} < V_2$. At smaller values of operating voltage that fall out of this domain but inside the NDR region, $V_1 < V_{GO} < V_{B1}$, the trains of the EHF pulses are self-excited (P-domain). At greater values, $V_{B2} < V_{GO} < V_2$, the CW oscillations are generated (C-domain).

The effect means bistability of the oscillation modes in the PC-domain. The kind of the mode being excited depends on the history of bias variations, i.e., on the way the oscillator is driven to the operating voltage. In this process, the oscillator reveals an hysteresis in switching between different modes. When the oscillator is driven into the PC-domain through the P-domain starting from small values, the EHF pulses are self-excited. On the contrary, when the oscillator is driven through the C-domain starting from large values, the CW oscillations are generated.

The PC-domain borders also depend on the direction of driving the operating voltage into this domain. So, there are, in fact, two kinds of P, C, and PC domains, which could be labeled, e.g., as P-up and P-down, C-up and C-down, and PC-up and PC-down domains. The effect is illustrated in **Figure 3** that shows the I-V curve of the Gunn diode in relative units $G(e)$ and the relevant domains of different oscillation modes.

Depending on the speed of driving the diode into the relevant stable domain of either the P or C kind, one can excite initially the oscillation mode, which is not intrinsic for that domain, e.g., CW oscillations in the P-domain. This mode is, however, unstable and after a certain period of time it gradually turns into the mode, which is intrinsic for the given domain, e.g., into the pulse mode in P-domain. Similarly, pulses, which could initially be excited in C-domain, gradually transform into the CW oscillations, which remain stable in this domain. The latter process is illustrated in **Figure 4**.

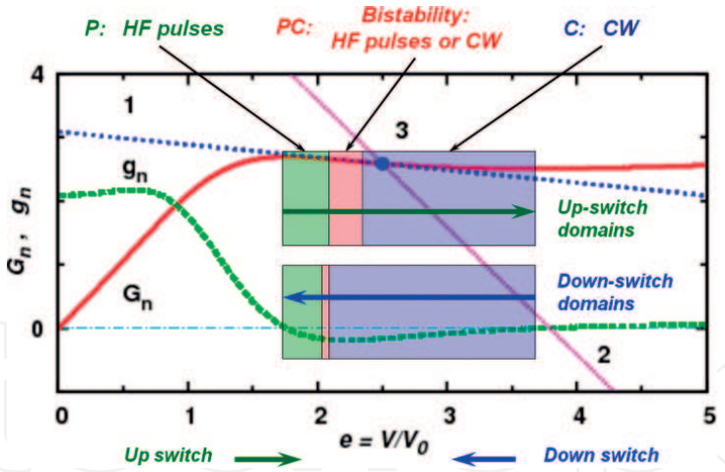

Figure 3.
Gunn diode current-voltage characteristics $G_n(e)(n = 1)$, differential conductance $g_n(e) = dG_n(e)/de$, two options for the load lines (curves 1 and 2), the operation point 3, and the voltage regions P, C, and PC, that correspond to the emergence of different oscillation modes in the NDR region $e_1 < e < e_2$ ([20]; licensed under a creative commons attribution (CC BY) license).

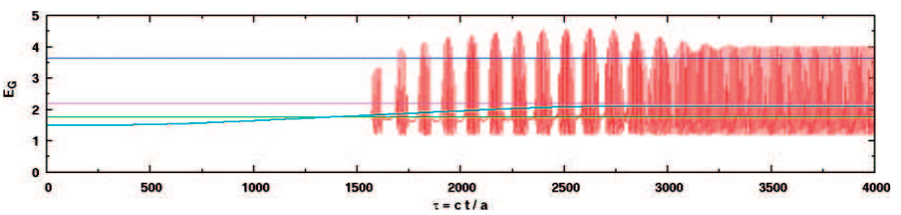

Figure 4.
Transition from the initial pulses to CW oscillations in the circuit with $d = 20$ at a very slow switching the bias voltage up to $e_B = 2.1$ in the C-up domain ([20]; licensed under a creative commons attribution (CC BY) license).

Let us now consider the properties and the mechanism of emergence of the EHF pulses. The time length of each pulse t_P appears to be equal to the interval of time between pulses Δt_P and each of them is equal to the time of the return trip of the EM signal between the active block G_1 to the resonator A_0. Thus, the EM pulse length $L_P = ct_P$ is twice the length of microstrip section connecting the Gunn diode and the resonator, $L_P = 2D$ at $t_P = \Delta t_P = 2D/c$.

The pulse carrier frequency ω is defined by the intrinsic frequencies of both the active block ω_G and the resonator ω_A. The condition for the emergence of a clear train of pulses is the coincidence of frequencies ω_G and ω_A. The length D of microstrip section has to be sufficiently large for the pulse duration t_P to be much greater than the oscillation period $T = 2\pi/\omega$. An example of a perfect train of the EHF pulses is shown in **Figure 5**.

In relative units, our simulations were made, typically, at the parameter values $\omega_A = \omega_G = 1$, $\omega_{C_A} = \omega_C = 10$, $\omega_{L_A} = \omega_L = 0.1$,$G_0 = 2$, and the microstrip length d chosen in the range of $d = 10 - 200$. The emerging radiation wavelength in relative units was $\lambda \approx 8$. When the normalization length a is chosen to be $a = 1$ mm, this corresponds to the oscillation frequency of $f \approx 37.5$ GHz. Then, $\omega_C = 10$ and $\omega_L = 0.1$ at $Z_0 = 50$ Ohm correspond to the capacitance $C = 0.07$ pF and the inductance $L = 0.17$ nH.

The emergence of one or another oscillation mode depends on the length d of the microstrip section between the Gunn diode and the remote resonator. The longer is the section, the easier trains of pulses are excited. Since the oscillations arise and decay at a very short time, the emergence of short pulses is possible at sufficiently short values of d, e.g., $d = 10$ at the wavelength $\lambda = 8$.

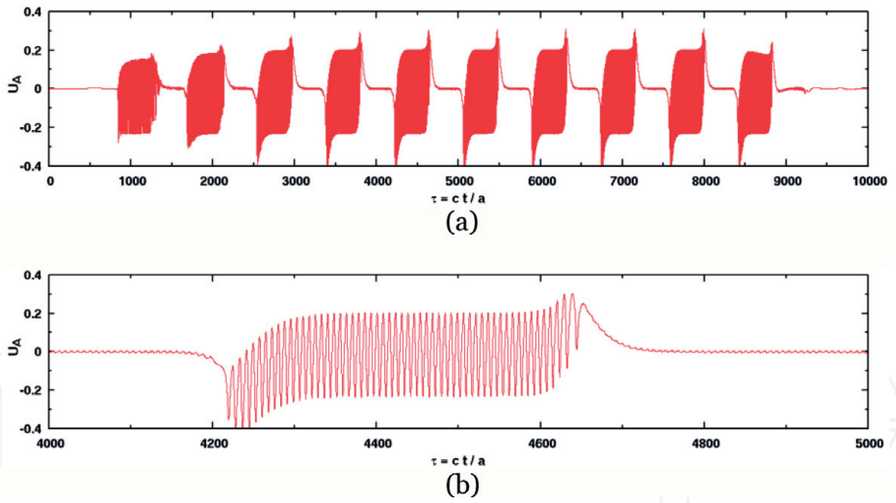

Figure 5.
(a) Train of the EHF pulses and (b) the shape of a single pulse generated by the circuit with $d = 200$ *at the oscillation period* $T \approx 8$ *when switching the bias voltage up to* $e_B = 2.0$ *at the rise-time* $T_R \approx 400$ *([20]; licensed under a creative commons attribution (CC BY) license).*

The formation of trains of the EHF pulses can be explained as follows. If the circuit is designed so that excitation is possible with no resonator at the site A_0, the oscillations appear and continue for the time t_P until the feedback signal returns from the resonator to the active block.

Then, if the conditions are so that oscillations cannot exist with both the active block and the remote resonator engaged, the oscillations cease for the period of time Δt_P when the active block receives a feedback signal and, therefore, "feels" the presence of the resonator. After that period of time, the feedback disappears, the active block does not "feel" any resonator again, and a new pulse of oscillations arises.

If the system is so that oscillations can exist in the presence of resonator, the oscillations, once appeared, would continue as a steady-state process. In this case, CW oscillations are excited whose frequency is defined by the Gunn diode and the remote resonator circuits.

The effects described above are tightly connected to a general problem of oscillation quenching and collective behavior of oscillators [29]. They are also related to bifurcations observed in square-wave switching in delay-coupled semiconductor lasers [30]. It is clear that, despite essentially different governing equations, the common feature of time-delay coupling leads to similar consequences in terms of nonlinear dynamics of microwave oscillations and optical polarization in these cases.

The generation of trains of pulses discussed above is obtained in the model that accounts for non-instant response of devices caused by the capacitance and inductance of active units [20]. These simulations confirm the conclusions of a simpler model [19] that the excitation of trains of the EHF pulses is a generic property of those oscillators, which are specified by remote location of their resonator structures.

7. Parallel and series connections of active circuits

One can imagine many kinds of active circuits and distributed networks of microstrip connected discrete circuits. There are two basic types of connection of active circuits, which are the parallel and series connections, **Figures 6** and 7, respectively.

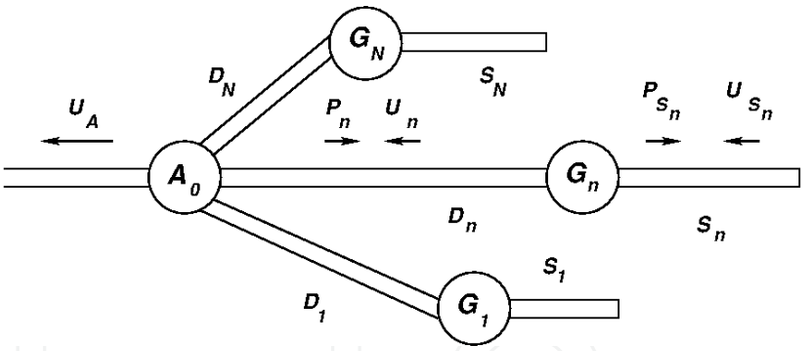

Figure 6.
Schematics of a parallel connection of active circuits where, in distinction from [21], different lengths of all microstrip sections D_n and stubs S_n are assumed as needed for quasi-chaotic oscillations.

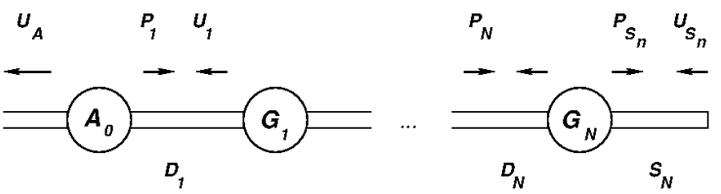

Figure 7.
Schematics of a series connection of active circuits where, unlike the case in [22], different lengths of different sections D_n are considered.

The parallel connection [21] is conceptually similar to the case of microwave cavity coupling of devices with spatial power combining considered by Kurokawa [6]. Spatial power combining is an important issue in this topic [31]. Our time-domain simulations of microstrip circuits connected in parallel confirm a possibility of increasing the total power output of the system proportional to the number of circuits N until a certain limiting value $N_{\max}$. At the same time, as typical for the circuits with a remote resonator A_0 connected to the active blocks G_n, trains of the EHF pulses can also be generated in these circuits.

The series connection of active circuits was also considered and the effect of nonlinear power combining was demonstrated [22]. The series connection of circuits appears to be less promising then the parallel connection since, due to the self-consistent evolution of the entire system, the basic oscillation frequency, typically, decreases with increasing the number of devices. The active blocks in [22] were different from those in [21] that, partially, could explain the effect. Nonetheless, the increase of the total length of the system in series connection is supposed to be the main reason of reducing the basic oscillation frequency.

Turning back to the parallel connection of active circuits and keeping in mind the explanation of the effect of pulsing presented in Section 6, we can consider a network of N parallel time-delay branches of Gunn diode circuits with different lengths of microstrip sections D_n [23]. With account of different times of arriving of time-delayed feedbacks in different branches and strong nonlinear mixing of oscillations in active devices, we can expect the development of complicated and, potentially, chaotic or quasi-chaotic oscillations.

As a test of this possibility, we considered a system of two parallel branches of identical active circuits presented in **Figure 2**, though of different and, generally, non-commensurable length of time-delay microstrip sections [23]. In this case, despite an apparent simplicity of the system, we observed complicated and, in the lower frequency bands, virtually quasi-chaotic nonlinear oscillations, **Figure 8**.

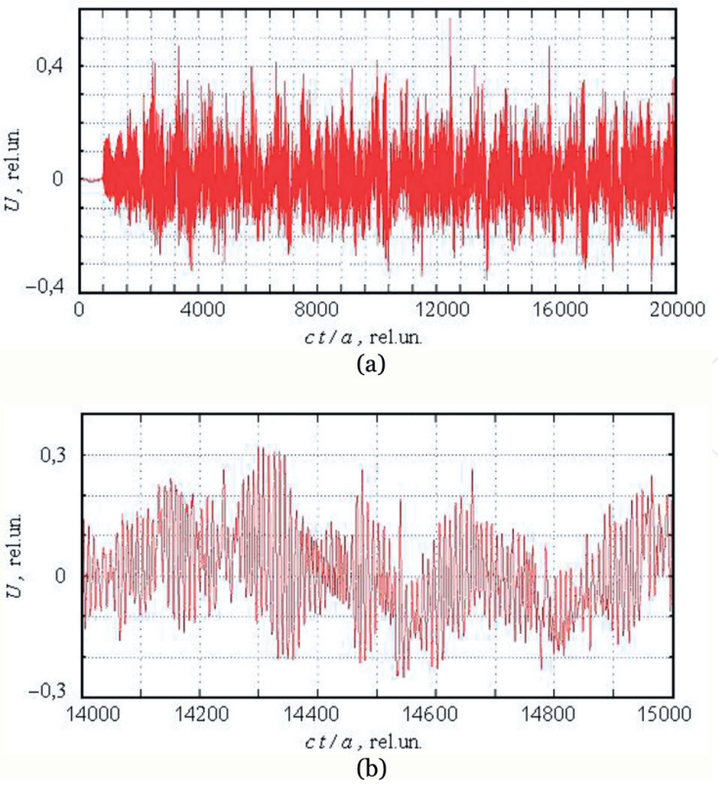

Figure 8.
(a) A quasi-chaotic signal radiated from a system of two Gunn diode circuits connected in parallel to the resonant antenna node by microstrip sections of the length $d_1 = 200$ and $d_2 = 266.67$, respectively, when the basic radiation wavelength is $\lambda = 8.6$ and (b) the close-up view of a part of this signal [23].

The effect is similar to the excitation of chaos in the 2D cavity [17, 18] or in the network of dispersive transmission lines where different frequency components take different times for the return of the feedback signal.

Quasi-chaotic character of the radiated wave in the low-frequency band was observed in both the Poincare sections and the auto-correlation functions of the emerging self-oscillations. When comparing auto-correlation functions of trains of the EHF pulses and quasi-chaotic signals arising under the relevant conditions, one can see a revival of correlations over the period of pulse repetition in the train of pulses and, on the contrary, a significant loss of correlation in the quasi-chaotic signal at all the times exceeding the basic period of oscillations, **Figure 9**.

Poincare sections plotted for the variables $U_A(\tau)$ and $dU_A(\tau)/d\tau$ show the presence of periodicity in the train of the EHF pulses and the lack of long-term periodicity in quasi-chaotic signals, **Figure 10(a)** and **(b)**, respectively.

The frequency spectrum of the quasi-chaotic signal shows the presence of chaotic components around the basic oscillation frequency and in the low-frequency band, **Figure 11**.

When the trains of the EHF pulses are excited, one can obtain rather short length of pulses. Since the process of turning on and off the EHF oscillation pulses is very short, one can obtained pulses that consist of just a few oscillations within each pulse when the microstrip sections between active circuits and resonant structures are sufficiently small, still being of nonzero length.

As an example, in a single-branch circuit of the kind shown in **Figures 1** and **2**, in case of $\omega_A = \omega_G = 1$, $\omega_{C_A} = 10$, $\omega_L = 0.1$ ($\omega_{L_A} = {\omega_A}^2/\omega_{C_A} = 0.1$, $\omega_C = {\omega_G}^2/\omega_L = 10$), $S = 0$, $R_A = R = 0$, and $G_0 = 2$, only two and four oscillations within each pulse were excited when the length of the microstrip section was $d = 10$ and $d = 20$, respectively, and the radiation wavelength was $\lambda \approx 8$.

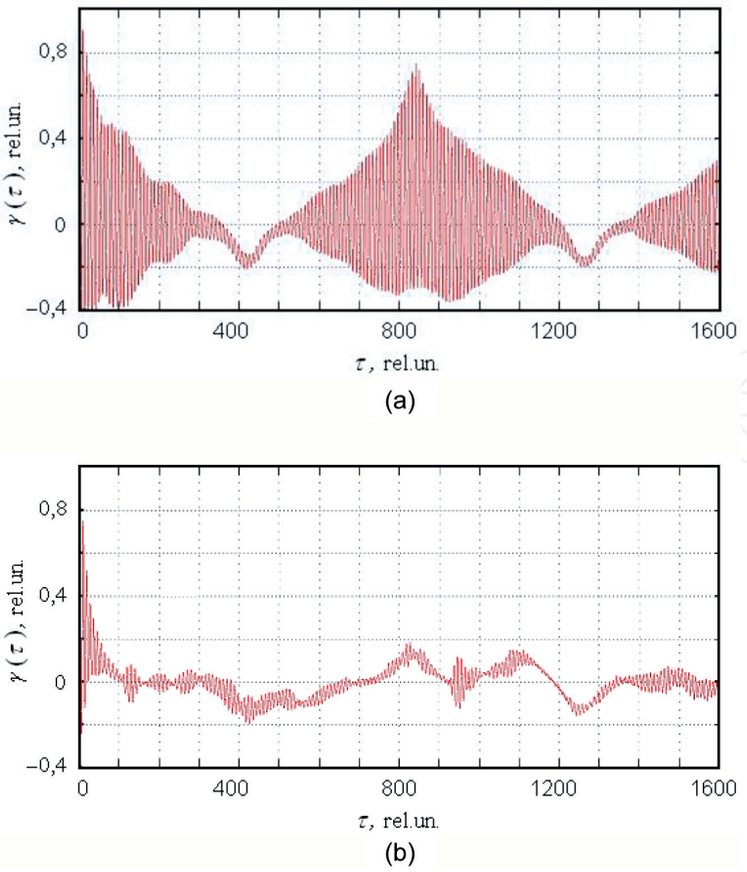

Figure 9.
Auto-correlation function of (a) train of pulses of the kind as shown in **Figure 5** *and (b) quasi-chaotic signal of* **Figure 8** *computed over the time interval* $\tau = 1000 - 9000$ *and* $\tau = 2000 - 20000$, *respectively [23].*

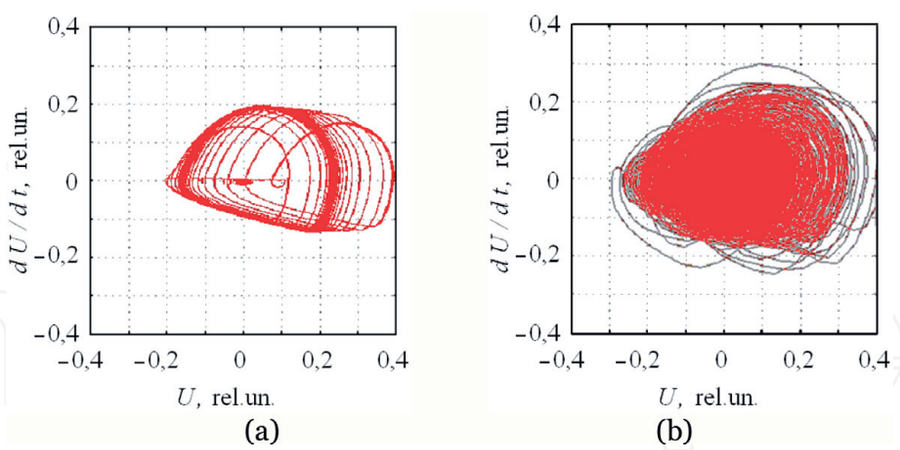

Figure 10.
Poincare sections of (a) pulsed and (b) quasi-chaotic signals processed in **Figure 9** *[23].*

One of the oscillators of such a kind was subject to the frequency-domain analysis for the comparison with time-domain simulations [24]. The oscillator had a single active block, though of slightly different design from those above, and a stub of length *S*. The analysis followed the ideas of the Kurokawa approach when applied to an open radiating circuit.

The frequency-domain analysis in the form adjusted for the radiating circuits was found to be capable of predicting small-signal oscillation spectra in either single- or multi-frequency cases [24]. At the same time, the approach, naturally, failed when strong nonlinear oscillations of more complicated character have been developed.

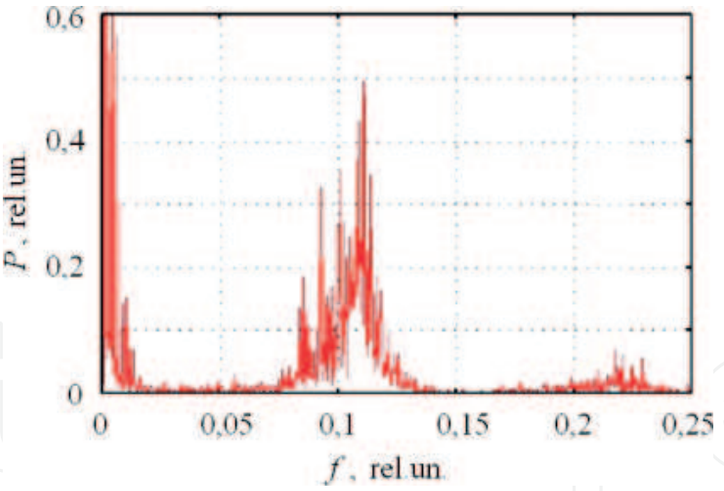

Figure 11.
Frequency spectrum of the waveform presented in **Figure 8** *[23].*

8. Resonant tunneling diode and laser diode circuit emitting trains of correlated EHF and optical pulses

Finally, we consider a time-delay version of an interesting oscillator that uses the laser diode driven by the resonant tunneling diode. The original form of the oscillator was proposed in [32, 33]. The RTD-LD circuit could generate optical (infrared) LD signals (pulses, oscillations, or chaos) when the RTD was excited by the external radio frequency (RF) bias. The authors made up the oscillator operating at the frequencies up to 2 GHz [33] and analyzed it with numerical simulations as a lumped unit.

The LD used in [33] was an optical communication laser operating at around 1550 nm IR radiation wavelength with an average output power of 5 mW. The RTD-LD hybrid circuit was produced with a minimal length of bonding wires b accessible with manual manufacture ($b \sim 1$ mm) so as to minimize the inductance of the system. Using the RTDs of small capacitance, the authors observed self-oscillations at the frequencies of 350–400 MHz, 550–590 MHz, and 1.82–2.17 GHz, depending on the bonding wire length b and other parameters. The authors made numerical simulations of their lumped oscillators and obtained a sufficiently good coincidence with experimental results [33]. The lumped circuit model is perfectly valid at these oscillator sizes and oscillation frequencies.

We considered a distributed version of the circuit that transforms the latter into an open system of the kind as shown in **Figures 1** and **2** of Sections 5 and 6, where the Gunn diode is replaced by a monolithic RTD-LD unit and the remote resonator block A_0 is used as a resonant antenna [25]. At the non-zero length D of the microstrip section connecting the RTD-LD unit and the resonant antenna, the circuit operates as a time-delay oscillator in a self-excitation mode when the RTD bias voltage falls in the NDR domain of the RTD unit.

Under the oscillation conditions, when using appropriate values of circuit parameters and, particularly, choosing the RTD operating at sufficiently high frequencies, e.g., up to 1 THz [34, 35], one can make the circuit to generate a train of short EHF pulses U_A, which are emitted into an open microstrip section and, eventually, radiated into the free space. At the same time, if the LD is also a high-speed device [36], a similar train of optical pulses would be emitted, which are correlated in a perfectly synchronous manner with original EHF pulses.

The trains of both the EHF and optical pulses can be rapidly turned on and off by the external bias digital signal applied to the RTD so as to produce relatively short

pieces of trains of EHF pulses. This property, along with a possibility of synchronous generation of both the EHF and optical pulses, can make the dual EHF-optical oscillators of this kind attractive for potential applications in various forms of close range radar systems. The optical power output of these systems can be increased when making reasonably large chip-on-board LD arrays of, e.g., 20 elements or so in a way similar to conventional high-power LED arrays.

There is an optimal range of the length of microstrip section D when the oscillator generates both the optical and EHF pulses being of a good shape, at the maximum EHF frequency, and the maximum light intensity. For example, at the device frequency $f_G = f_A = 7.6$ GHz, the entire range where the effect exists is $D = 1 - 20$ mm and the optimal D is about $D = 5$ mm ($d = 5$ at the unit length $a = 1$ mm).

In addition to the basic form of dual EHF-optical pulse oscillations presented above, there is another, a more interesting mode of operation. When having a sufficiently large excess in the operation speed of the RTD-LD unit as compared to the duration of separate pulses, each optical pulse can also be modulated in power by the RTD EHF current. This makes both the EHF and optical pulses carrying the same EHF signal, **Figure 12**.

Figure 12 shows an example of the EHF pulse radiated by the RTD-LD circuit and the relevant EHF-modulated optical pulse. Pulse oscillations have been computed when both the RTD-LD and the resonator circuit intrinsic frequencies are $f_G = f_A = 76$ GHz assuming $\omega_C = \omega_{C_A} = 1$, $\omega_L = \omega_{L_A} = 1$, and $d = 1$. In this case, the LD electron lifetime parameter is chosen to be $t_n = 10$ ps so that the LD optical output could follow more frequent oscillations of the RTD circuit. These values assume sufficiently small capacitance and inductance of the devices. At the given parameters, they should be about $C = C_A = 55$ fF and $L = L_A = 80$ pH. Despite being extremely small, these values become accessible with modern RTD technology [34, 35]. When using, instead, the parameters $\omega_C = \omega_{C_A} = 10$ and $\omega_L = \omega_{L_A} = 0.1$, we get $C = C_A = 5.5$ fF and $L = L_A = 0.8$ nH that makes, possibly, a more realistic system. In this case, we can produce a single oscillation within a pulse and a short burst of the EHF oscillations at the pulse length $t_P = 25$ ps and $t_P = 50$ ps, respectively [25].

Detection of the EHF modulation of optical (IR) pulses is yet another issue. Direct detection of the EHF modulation of optical pulses is expected to become possible with an RF optical heterodyne photo-detector proposed in [37].

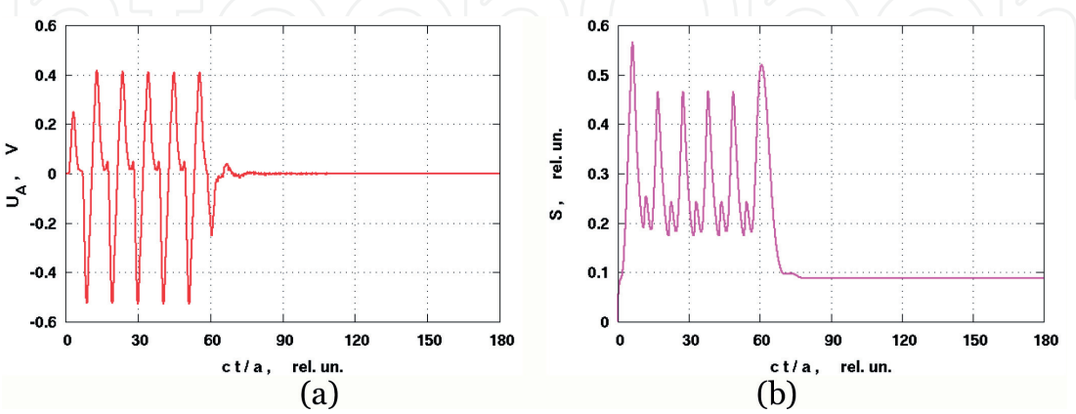

Figure 12.
Excitation of (a) the EHF pulse and (b) the EHF-modulated optical pulse when $G_0 = 0.5$, $d = 1$, $f_G = f_A = 76$ GHz, and $t_P = 0.2$ ns [25].

9. Conclusions

We presented time-domain simulations of distributed time-delay oscillators, which show complicated nonlinear dynamics of electromagnetic oscillations generated by these systems.

We considered the models that consist of discrete lumped circuits of active and passive devices and distributed sections of microstrip lines connecting the lumped circuits. The active devices were presented by the Gunn diodes and the resonant tunneling diodes operating in the EHF frequency band. Parallel and series connections of microstrip sections with active devices have been simulated. Other structures like a 2D microwave cavity with a wall covered with active devices and a 1D open resonator made by a similar wall and a thin dielectric mirror have also been investigated.

Simulation models were developed, which rely on the method that reduces the problems for the wave equations in structures with active devices to the problems with time-delay equations of difference-differential kind. A Dormand-Prince method of the (5,3) order of accuracy for ordinary differential equations was applied and extended for solving time-delay equations arising in simulation.

Time-domain simulations revealed a diversity of dynamical effects in time-delay oscillators being considered. A possibility of chaotic or quasi-chaotic oscillations was observed in a 2D cavity with active devices and in some cases of parallel connection of microstrip sections with Gunn diode circuits.

Self-excitation of trains of the EHF pulses in microstrip structures with Gunn diodes and remote resonators have been discovered. A similar kind of trains of either the baseband or the EHF pulses were also observed in a more simplified model of a 1D cavity with an active layer and a dielectric mirror. Bistability in the generation of either the continuous waves or the trains of the EHF pulses in the Gunn diode systems with remote resonator was discovered and hysteresis in switching between these generation modes was observed.

A dual kind of the EHF-pulse and the EHF-modulated optical pulse generator using an RTD-LD time-delay oscillator has been proposed and investigated.

The approach based on the splitting of oscillator systems on discrete parts of active circuits and distributed parts of propagation sections makes it possible time-domain simulations of complex oscillatory structures. The approach has a major advantage over exact modeling with common engineering software. It allows one to address the problems of time-domain simulation of distributed systems with limited computational resources. This makes the analysis of this kind of systems feasible that, otherwise, would be out of reach with conventional simulation tools.

Acknowledgements

This work was funded in part by NATO research projects NUKR.SFPP 985465 (G5465) and NUKR.SFPP 985395 (G5395) within 37 frames of the Science for Peace and Security (SPS) program.

Author details

Vladimir Yurchenko* and Lidiya Yurchenko
O. Ya. Usikov Institute for Radiophysics and Electronics, National Academy of Sciences of Ukraine, Kharkiv, Ukraine

*Address all correspondence to: v.yurchenko.nuim@gmail.com

IntechOpen

References

[1] Lukin K. Noise radar technology. Telecommunications and Radio Engineering. 2001;**55**(12):8-16. DOI: 10.1615/TelecomRadEng.v55.i12

[2] Lukin K. Millimeter-wave band noise radar. Telecommunications and Radio Engineering. 2009;**68**(14):1229-1255. DOI: 10.1615/TelecomRadEng.v68.i14.20

[3] Golio M, editor. The RF and Microwave Handbook. Boca Raton: CRC Press LLC; 2000. 1376 p. ISBN 9781420036763

[4] Grebennikov A. RF and Microwave Transistor Oscillator Design. Chichester: Wiley; 2007. 441 p. DOI: 10.1002/9780470512098

[5] Kurokawa K. Noise in synchronized oscillators. IEEE Transactions on Microwave Theory and Techniques. 1968;**16**:234-240. DOI: 10.1109/TMTT.1968.1126656

[6] Kurokawa K. The single-cavity multiple-device oscillator. IEEE Transactions on Microwave Theory and Techniques. 1971;**19**:793-801. DOI: 10.1109/TMTT.1971.1127642

[7] Vendelin G, Pavio A, Rohde U. Microwave Circuit Design Using Linear and Nonlinear Techniques. Chichester: Wiley; 2005. 1058 p. DOI: 10.1002/0471715832

[8] Gonzalez-Posadas V, Jimenez-Martin J, Parra-Cerrada A, Segovia-Vargas D, Garcia-Munoz L. Oscillator accurate linear analysis and design. Classic linear methods review and comments. Progress in Electromagnetics Research. 2011;**118**:89-116. DOI: 10.2528/PIER11041403

[9] Erturk V, Rojas R, Roblin P. Hybrid analysis/design method for active integrated antennas. IEE Proceedings Microwave Antennas Propagation. 1999; **146**(2):131-137. DOI: 10.1049/ip-map:19990208

[10] Rao S. Time Domain Electromagnetics. San Diego: Academic Press; 1999. 372 p. DOI: 10.1016/B978-0-12-580190-4.X5000-9

[11] Aksoy S, Tretyakov O. Evolution equations for analytical study of digital signals in waveguides. Journal of Electromagnetic Waves and Applications. 2003;**17**(12):1665-1682. DOI: 10.1163/156939303322760209

[12] Sirenko Y, Strom S, Yashina N. Modeling and Analysis of Transient Processes in Open Resonant Structures. New York: Springer; 2007. 353 p. DOI: 10.1007/0-387-32577-8

[13] Asakawa K, Itagaki Y, Shi-Ya H, Saito M, Suhara M. Time-domain analysis of large-signal-based nonlinear models for a resonant tunneling diode with an integrated antenna. IEICE Trans. on Electronics. 2012;**E95-C**(8):1376-1384. DOI: 10.1587/transele.E95.C.1376

[14] Coillet A, Henriet R, Salzenstein P, Huy KP, Larger L, Chembo YK. Time-domain dynamics and stability analysis of optoelectronic oscillators based on whispering-gallery mode resonators. IEEE Journal of Selected Topics in Quantum Electronics. 2013;**19**(5):6000112. DOI: 10.1109/JSTQE.2013.2252152

[15] Anzill W, Russer P. A general method to simulate noise in oscillators based on frequency domain techniques. IEEE Trans. on Microwave Theory and Techniques. 1993;**41**(12):2256-2263. DOI: 10.1109/22.260715

[16] Atay F, editor. Complex Time-Delay Systems. Berlin: Springer-Verlag; 2010. 322 p. DOI: 10.1007/978-3-642-02329-3

[17] Yurchenko L, Yurchenko V. Noise generation in a cavity resonator with a wall of solid-state power-combining array. In: Proceedings of the 11th International Conference on Microwaves and Radar (MIKON-96); 27-30 May 1996; Poland. Vol. 2. Warsaw: IEEE; 1996. pp. 454-458

[18] Yurchenko L, Yurchenko V. Analysis of the dynamical chaos in a cavity with an array of active devices. In: Proceedings of the 12th International Conference on Microwaves and Radar (MIKON-98); 20–22 May 1998; Poland. Vol. 3. Krakow: IEEE; 1998. pp. 723-727

[19] Yurchenko L, Yurchenko V. Self-generation of ultra-short pulses in a cavity with a dielectric mirror excited by an array of active THz devices. In: Proceedings of the 8th International Conference on Terahertz Electronics. 28–29 September 2000, Darmstadt, Germany; 2000. pp. 49-52

[20] Yurchenko V, Yurchenko L. Bistability and hysteresis in the emergence of pulses in microstrip Gunn-diode circuits. AIP Advances. 2014;**4**:127126. DOI: 10.1063/1.4904226

[21] Yurchenko L, Yurchenko V. Time-domain simulation of power combining by a parallel connection of strip lines with Gunn diodes. Telecommunications and Radio Engineering. 2014;**73**(5): 375-390. DOI: 10.1615/TelecomRadEng.v73.i5.10

[22] Yurchenko V, Yurchenko L. Time-domain simulation of power combining in a chain of THz Gunn diodes in a transmission line. International Journal of Infrared and Millimeter Waves. 2004;**25**(1):43-54. DOI: 10.1023/B:IJIM.0000012761.27947.01

[23] Yurchenko L, Yurchenko V. Time-domain simulation of short-pulse oscillations in a Gunn diode system with time-delay microstrip coupling. Applied Radio Electronics. 2013;**12**(1):45-50. Print ISSN 1727-1290

[24] Yurchenko V, Yurchenko L. Self-excitation of a chain of Gunn diodes connected by transmission lines. In: Proceedings of the 2nd URSI-Turkey'2004 Symposium; 8–10 September 2004; Turkey, Ankara: URSI; 2004. pp. 460-462

[25] Yurchenko V, Yurchenko L, Ciydem M. Pulse-mode simulations of RTD-LD circuits for visible light communication. Applied Radio Electronics. 2018;**17**(1-2): 66-71. Print ISSN 1727–1290

[26] Hairer E, Wanner G. Solving Ordinary Differential Equations II: Stiff and Differential-Algebraic Problems. 2nd ed. Berlin: Springer-Verlag; 1996. 609 p. DOI: 10.1007/978-3-662-09947-6

[27] SmartSpice. [Internet]. 2018. Available from: https://www.silvaco.com/products/analog_mixed_signal/smartspice_46.pdf [Accessed: 2018-09-24]

[28] Yurchenko V, Ciydem M, Gradziel M, Yurchenko L. MM-wave dielectric parameters of magnesium fluoride glass wafers. Progress in Electromagnetics Research. 2017;**62**:89-98. DOI: 10.2528/PIERM17081805

[29] Zou W, Senthilkumar D, Duan J, Kurths J. Emergence of amplitude and oscillation death in identical coupled oscillators. Physical Review E. 2014;**90**: 032906. DOI: 10.1103/PhysRevE.90.032906

[30] Masoller C, Sukow D, Gavrielides A, Sciamanna M. Bifurcation to square-wave switching in orthogonally delay-coupled semiconductor lasers: Theory and experiment. Physical Review A. 2011;**84**:023838. DOI: 10.1103/PhysRevA.84.023838

[31] DeLisio M, York R. Quasi-optical and spatial power combining. IEEE Transactions on Microwave Theory and

Techniques. 2002;**50**(3):929-936. DOI: 10.1109/22.989975

[32] Slight T, Romeira B, Wang L, Figueiredo J, Wasige E, Ironside C. A Lienard oscillator resonant tunnelling diode-laser diode hybrid integrated circuit: Model and experiment. IEEE Journal Quantum Electronics. 2008; **44**(12):1158-1163. DOI: 10.1109/JQE.2008.2000924

[33] Romeira B, Figueiredo J, Slight T, Wang L, Wasige E, Ironside C, et al. Synchronisation and chaos in a laser diode driven by a resonant tunnelling diode. IET Optoelectronics. 2008;**2**: 211-215. DOI: 10.1049/iet-opt:20080024

[34] Suzuki S, Asada M, Teranishi A, Sugiyama H, Yokoyama H. Fundamental oscillation of resonant tunneling diodes above 1 THz at room temperature. Applied Physics Letters. 2010;**97**(24):242102. DOI: 10.1063/1.3525834

[35] Feiginov M, Sydlo C, Cojocari O, Meissner P. Resonant-tunnelling-diode oscillators operating at frequencies above 1.1 THz. Applied Physics Letters. 2011;**99**:233506. DOI: 10.1063/1.3667191

[36] Tsonev D, Videv S, Haas H. Towards a 100 Gb/s visible light wireless access network. Optics Express. 2015;**23**(2):1627-1637. DOI: 10.1364/OE.23.001627

[37] Li Q, Sun K, Li K, Yu Q, Runge P, Ebert W, et al. High-power evanescently coupled waveguide MUTC photodiode with > 105-GHz bandwidth. Journal of Lightwave Technology. 2017; **35**(21):4752-4757. DOI: 10.1109/JLT.2017.2759210